doi.org/10.36721/PJPS.2026.39.4.REG.14749.1

Unfolding protection: *Terminalia arjuna* targets UPR pathways to counteract ER stress in hepatotoxicity

Wania Nasir[1], Shamshad Ul Hassan[1]*, Bilal Aslam[1] and Wafa Majeed[2]
[1]Institute of Physiology and Pharmacology, Faculty of Veterinary Science, University of Agriculture Faisalabad, Pakistan
[2]Department of Pharmacy, Faculty of Health and Pharmaceutical Sciences, University of Agriculture Faisalabad, Pakistan

Abstract: **Background**: Drug-induced liver injury (DILI) from acetaminophen (APAP) overdose involves ER stress, oxidative damage, apoptosis, and inflammation. **Objective**: This study assesses *Terminalia arjuna* bark extract (TAE) against APAP-induced toxicity in rats, comparing its efficacy with N-acetylcysteine (NAC) through key signaling and inflammatory markers. **Methods**: Twenty-four Wistar rats were equally divided into four groups: Control Negative (CN, no treatment), Control Positive (CP, acetaminophen 350 mg/kg), N-acetylcysteine (NAC, 150 mg/kg), and *Terminalia arjuna* bark extract (TAE, ethanolic, 80 mg/kg). Over 14 days, liver injury was induced in the CP group via acetaminophen, while the NAC and TAE groups received their respective treatments. Animals were decapitated on day 15, and biological samples were collected for analysis. Biochemical assessments included liver function markers (ALT, AST) and oxidative stress parameters (SOD, TAC, TBARS, TOS). Gene expression studies were performed for oxidative stress regulators (Keap1, Nrf2) and ER stress signaling molecules (ERK, JNK, PPAR-α, AKT). Histopathological examination evaluated liver architecture and cellular integrity. **Results**: Acetaminophen induced significant hepatotoxicity, as reflected by elevated liver enzymes, increased oxidative stress, altered gene expression, and disrupted liver histology. APAP toxicity resulted in elevated oxidative stress, apoptosis, inflammation, and ER stress, leading to significant hepatic damage ($p < 0.0001$ vs CN). NAC and TAE treatments mitigated these effects, with TAE demonstrating superior improvement in oxidative stress markers ($p < 0.0001$ vs CP). Gene expression analysis revealed a protective shift in the Keap1-Nrf2 pathways in the treated groups. Histopathology confirmed reduced necrosis and preserved hepatic architecture in the NAC and TAE groups. **Conclusion**: *T. arjuna* exhibits potent hepatoprotective effects, comparable to NAC, through modulation of oxidative stress, apoptosis, and ER stress pathways. Further studies are needed to explore its clinical applicability in acute liver injury management.

Keywords: Adaptive ER signaling; Hepatic remodeling; Herbal intervention; Modulation pathways; Mitochondrial stabilization; Phytochemical cryoprotection; Proteostasis; Redox remedy

Submitted on 16-06-2025 – Revised on 07-08-2025 – Accepted on 11-08-2025

INTRODUCTION

Hepatic Physiology relates to the mechanisms by which the liver metabolizes organic and inorganic products for either absorption of essential metabolites or removal of waste from the body (Alamri, 2018). The cellular machinery responsible for dispensing organic and inorganic products into reusable reservoirs or excretory material faces the biggest challenge of toxicity by these products, leading to cellular stress and organ injury (Kong *et al*., 2023). The use of remedial elements often offers a valuable solution to such toxicity but is compromised when tolerance is built by the natural system against such therapeutic agents. Plant-based natural products are thus researched as plausible alternatives with higher treatment potential and fewer side effects (Rui, 2014).

Drug-induced Liver Injury (DILI) is a clinically renowned terminology used by physicians to define the damage inflicted upon the liver due to drug overdose. Clinically and pathologically, it can show up as a variety of symptoms, from asymptomatic liver dysfunction to acute liver failure (ALF) and death. DILI can mimic other forms of liver diseases, making it important to consider in the differential diagnosis of any liver disease (Hosack *et al*., 2023). According to the statistical and demographic data on hospital admissions per annum, DILI accounts for the most OPD admissions, liver transplantation requests and immediate drug withdrawal and discontinuation (Katarey and Verma, 2016). The progression of liver injury due to drug misuse or overdose is brought upon by three principal approaches; direct effects of active drug on hepatocytes, indirect effect of secondary drug metabolites on hepatic homeostasis, or initiation of an immune response due to accumulation of toxic metabolic entities (Iorga *et al*., 2017). The clinical toxicity assays classify ALF due to drug overdose as (a) intrinsic/dose-dependent DILI, or (b) idiosyncratic/dose-independent DILI, where idiosyncrasy is not commonly observed in clinical practice and is a rare occurrence (Andrade *et al*., 2019).

Among all the OTC drugs, NSAIDs particularly APAP have been reported as the major cause of DILI-associated ALF. APAP overdose has been associated with frequent hospital admissions of ALF cases requiring liver transplantation (Chalasani *et al*., 2014). APAP is the choice of drug and most prescribed OTC for its antipyretic and

**Corresponding author:* e-mail: drshamshad.kalyar@uaf.edu.pk

analgesic effects in treating low-grade pyrexia. The overdose of APAP causes the accumulation of its toxic metabolites, which reduce natural cellular glutathione stores leading to the generation and abundance of ROS (reactive oxygen species) (Saito *et al*., 2010). The subsequent events lead to an imbalance in redox reactions that are necessary to evacuate toxic metabolites out of hepatocytes and thus the cells undergo ROS-mediated stress (Rao *et al*., 2015). These proteins are adaptive homeostatic modulators and are activated in response to prolonged ERS and loss of glutathione reservoirs (Uzi *et al*., 2013). Persistent cellular stress and ER damage lead to cells activating death caspases for immediate apoptosis, which clinically presents itself with the symptoms of ALF (Paridaens *et al*., 2017). ROS is produced excessively in the cells that the antioxidant system is unable to neutralize and is referred to as oxidative stress. In the body, ROS are typically created in small amounts and are essential for controlling many processes like signal transmission, gene expression and receptor activation that preserve cell homeostasis (Mandal *et al*., 2013). It is understood that the harmful effects on the liver caused by acetaminophen are triggered by the harmful byproduct of the cytochrome p450 system, N-acetyl-p-benzoquinone-imine (NAPQI) (Hu *et al*., 2019).

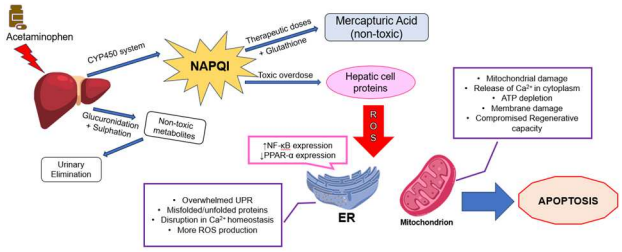

Fig. 1: Molecular pathophysiology of DILI by APAP-toxicity.

The scientific community has been researching plant-based organic products with bioactive ingredients that mimic the role of major human genomic pathways and play a role in modulating gene-protein expression in metabolic diseases. The therapeutic qualities of numerous plants have been well-documented in academic research. One such plant is the *Terminalia arjuna* tree, a member of the Combretaceae family with uses in ancient Ayurveda. Arjunolic acid (AA) is a chiral triterpenoid saponin and is considered to be the active ingredient in *T. arjuna* extracts studied for its phytochemical properties. Apart from AA, other principal bioactive components of arjuna extracts have also been studied for their efficacy in mitigating oxidative stress caused by excessive ROS and stress on cellular machinery (Ghosh *et al*., 2010). In biological systems, the effects of *T. arjuna* extracts and specifically the effects of AA have been studied in disease models of cardiac hypertrophy, nephritis and ROS-mediated hepatocellular fibrosis (Manna *et al*., 2006). The rationale of the current study is built upon the literature gap which has not yet elucidated the details behind the genetic interplay of DILI associated with APAP toxicity, upregulation of nuclear factors for apoptosis and downregulation of cell survival pathways.

MATERIALS AND METHODS

Experimental design and protocols

Study design

A total of 24 male albino Wistar rats (weighing ~200g) were obtained and housed in the Institutional Animal Facility under standard laboratory conditions (22 ± 2°C, 12-h light/dark cycle, with free access to standard rat feed and water). The experimental units were equally divided into four groups, namely Control Positive (CP), Control Negative (CN), Standard treatment (NAC) and Herbal treatment (TAE), with six rats in each group. The CN group received no induction or treatment. The CP group was administered an IP injection of acetaminophen (350mg/kg) dissolved in warm saline on day 1, day 7 and day 14. The NAC group was administered the same IP induction dose of acetaminophen, followed by an oral dose of N-Acetylcysteine (150mg/kg) dissolved in normal saline as standard treatment and administered using a nasogastric tube. Finally, the TAE group was treated with an oral dose of *T. arjuna* ethanolic extract (80mg/kg), maintaining standard feed and water *ad libitum* for all groups throughout the 14 days of the experimental trial. Experimental units from each group were decapitated on day 15 to obtain biological samples.

Plant identification and extraction

The plant of choice (*T. arjuna* bark) was botanically classified (Voucher No.1017-1-2023) and subjected to extraction protocols following the double extraction method with slight modifications (Manna *et al*., 2007). The bark was first soaked in petroleum ether for 24 hours to remove non-polar compounds. The supernatant was discarded and the remaining residue was extracted with 70% ethanol for the final treatment product (Ahmad *et al.,* 2025).

Ex-vivo biological assessments

The experimental units from each group were decapitated to obtain biological samples for serological testing, gene expression studies and histological imaging. Blood samples were collected in heparin-coated vacutainers for serum separation. Liver tissue samples were collected in formalin jars for histopathology and TRIzol™ (guanidinium isothiocyanate-phenol solution, chaotropic agent for nucleic acid separation) coated Eppendorf tubes for gene expression analysis.

Dose and toxicity assessments

The dose of acetaminophen (350 mg/kg, intraperitoneal) used in this study was adapted from Paridaens *et al*. (2017), slightly modified to suit the trial duration and required toxicity exposure while avoiding mortality. The LD_{50} for APAP toxicity in rats is variable according to age, weight

and strain of experimental unit and lies in a range of 700mg/kg - 1500mg/kg body weight (Green *et al*., 1984). Similarly, a variable range was researched for NAC lethality in rats, ranging from 400mg/kg - 800mg/kg body weight (Tsai *et al*., 2024). For N-acetylcysteine, a dose of 150 mg/kg was selected based on Sanabria-Cabrera *et al*. (2021), modified for a 14-day parallel treatment approach aimed at reducing hepatotoxic effects. The dose of *T. arjuna* ethanolic extract was derived from Mishra (2021), who reported using doses between 250 mg/kg and 500 mg/kg to evaluate its anti-inflammatory potential and effects on mitochondrial-dependent apoptotic signaling pathways.

Serology: Liver function tests

The serum was separated from blood by centrifugation in a refrigerated microcentrifuge (Hermle LaborTechnik - Model Z216-MK) at 5000 RPM for 5 minutes. The resultant serum was subjected to use with ELISA-based kinetic determination kits followed by spectrophotometry for liver function tests, mainly ALT (Bioclin Transaminase ALT Kinetic - Catalogue No. K049) and AST (Bioclin Transaminase ALT Kinetic - Catalogue no. K048). The spectrophotometer used for visualization was the Thermo Fisher Scientific Multi-Scan Spectrophotometer (Reference No. 51119300).

Serology: Oxidative stress tests and antioxidant markers

The separated sera of experimental units from each group were subjected to oxidant status analyses and antioxidant capacity tests based on enzymatic and colorimetry principles. All assay kits used were purchased from Elabscience®. The following kits were used: Superoxide Dismutase (SOD) Activity Assay Kit (Catalogue No. BC0175), Thiobarbituric Acid Reactants (TBARS) Colorimetric Assay Kit (Catalogue No. E-BC-K298-M), Total Antioxidant Capacity (TAC) Colorimetric Assay Kit (Catalogue No. E-BC-K801-M) and Total Oxidative Status (TOS) Colorimetric Assay Kit (Catalogue No. E-BC-K802-M).

Nucleic acid separation and gene expression analysis

Total RNA was extracted manually from the tissue samples preserved in TRIzol™ (Invitrogen™ Thermo Fisher Scientific - Catalogue No. 15596026), followed by phase separation and RNA precipitation. The RNA precipitate was washed and resuspended in Nuclease-free water (UltraPure™ DNase/RNase-Free Distilled Water - Catalogue No. 10977015). A multi-scan Spectrophotometer (Thermo Fisher Scientific - Reference No. 51119300) was used to assess the quality and concentration of obtained RNA using a µDrop Plate™ (Thermo Fisher Scientific - Catalogue No. N12391). Subsequently, complementary DNA (cDNA) was synthesized using the RevertAid First Strand cDNA Synthesis Kit (Molecular Biology Thermoscientific - Catalogue No. K1622) according to the manufacturer's instructions. Quantitative real-time PCR (qRT-PCR) was performed using Maxima SYBR Green/ROX qPCR Master Mix (Molecular Biology Thermoscientific - Catalogue No. K0221) to quantify gene expression levels in a thermal cycler (Bio-Rad CFX96 Touch Real-Time PCR Detection System - Serial No. 785BR15948) (Dogan *et al.,* 2025). The gene-specific primers to assess the role of oxidative stress genes, apoptotic, cell signaling and proliferative genes were designed using the Primer-BLAST tool on the NCBI online platform by setting genetic specificity and optimal annealing conditions. Suitable primers were selected, having the following forward and reverse sequences:

Oxidative stress regulation

Keap1 (F: 5'-GAGTGAAGTGACCCGCTTGA-3', R: 3'-CCCTTCGTGGAAGAAGGCAT-5'), Nrf2 (F: 5'-GGGAGTACCTCTTTTGGCCC-3', R: 3'-CACTGCAGCTCAGGTCAGAA-5').

UPR signaling pathway molecules

ERK (F: 5'-TCTCCTCTCCAGGGCTACAC-3', R: 3'-CTTCTGATCCGCTAACCCCC-5'), JNK (F: 5'-CCGCCAGTACAGAGAAGCTC-3', R: 3'-CCTGTCAGTGTCCTTCCCAC-5'), PPAR-α (F: 5'-CTGAGTCTAGCCACTGCTGG-3', R: 3'-GGGTAGCTTTGGCATCGTCT-5') and AKT (F: 5'-GGCGTGGTCATGTACGAGAT-3', R: 3'-GCAGCAGTACTGTCCAGAGG-5').

Histopathology

A neutral buffered (10%) formalin solution was prepared by dissolving 8g disodium hydrogen phosphate, anhydrous (Uni-Chem® - Catalogue No. S40250-4J) with 13g disodium hydrogen phosphate, dihydrate (AppliChem – Catalogue No. 10028-24-7) in 200 ml warm water and incorporating this mix with 1800 ml formaldehyde solution (1600ml water + 200ml formaldehyde). The biological tissue samples were immersed in formalin-filled sterile jars in a 1:20 ratio for proper tissue fixation. The fixed tissues were subjected to paraffin wax imbedding and staining protocols. The slides were stained with Hematoxylin and Eosin stain and visualized under a Lab-grade compound light microscope (IRMECO, Germany - Model IM-910) at different magnification powers.

Statistical analysis

All the numeric data was subjected to Analysis of Variance (ANOVA) followed by suitable post-significance tests for comparison between the means of groups. Data are expressed as Mean ± SEM (standard error of mean) with at least four determinations for each experimental group (n = 4). The difference at $P<0.05$ ($\alpha = 0.05$) was considered significant. The statistical software used for simple graphical analyses was GraphPad Prism (version 8.0.1, San Diego, CA).

RESULTS

Serology: Liver function tests

The hepatoprotective effects of *T. arjuna* bark extract on basic liver function markers that are primarily affected by changes in dietary patterns or by alterations in biotransformation reactions of the liver are shown in fig 2. The serum levels of ALT, AST and Total Bilirubin are shown. In the acetaminophen-treated group (CP), the serum levels of these enzymes were significantly higher compared to the control group (CN) ($p < 0.0001$), indicating hepatocytic damage due to leakage of these enzymes from the damaged cytosol of hepatocytes into the bloodstream. The subsequent significant increase ($p < 0.0001$) in total bilirubin also indicates elevated biliary function in the diseased state. The serum levels of these biomarkers in the *T. arjuna* extract-treated group significantly dropped compared to the CP group, which revealed the potent antihepatotoxic effects of *T. arjuna* extract in diminishing the toxic effects of acetaminophen. The standard treatment group (NAC) had a slightly significant ($p < 0.05$) and a non-significant relevance to the TAE group, indicating a radically similar therapeutic effect related to acetaminophen toxicity in the CP group.

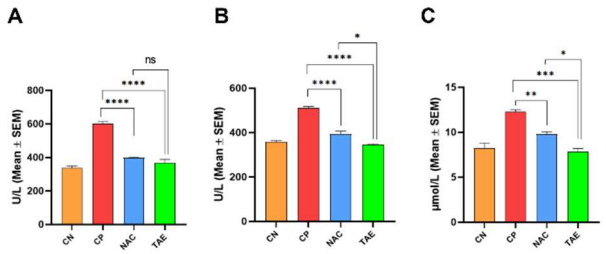

Fig. 2: Effects of different treatments on liver function tests.
(A) Alanine aminotransferase (ALT), (B) Aspartate aminotransferase (AST), and (C) Total bilirubin. Serum levels were measured to assess liver function across the experimental groups. Data are presented as Mean ± SEM. The CP group significantly increased all the parameters, indicating acute hepatic injury. Treatment with NAC and TAE significantly reduced ALT, AST, and bilirubin levels, implying the protective effects of treatment on the liver. *Statistical significance is denoted as *p<0.05, **p<0.01, ***p<0.001, ****p<0.0001, ns=p>0.05 (not significant)*

Serology: Oxidative stress tests and antioxidant markers

The overall cellular oxidative status is measured through biomarkers such as SOD, TBARS, TAC and TOS which are represented in fig. 3. Section (A) shows SOD activity across the experimental groups. A heightened oxidative burst is evident in the CP groups where a marked reduction of SOD activity is seen compared to the CN group ($p < 0.0001$). Both the treatment groups on the other hand showed a significant increase ($p < 0.001$) in SOD activity, suggesting the restoration of enzyme activity in these groups. However, the NAC group achieved a high SOD activity ($p < 0.001$ vs CP), suggesting its potent hepatoprotection in acetaminophen toxicity but the TAE group showed a higher SOD activity than NAC, which is indicative of a more pronounced effect of TAE in restoring antioxidant defenses. Section (B) shows TBARS levels across the experimental groups. TBARS is an oxidant-indicative marker and its high levels indicate oxidative damage due to lipid peroxidation (Tsai and Huang, 2015). In the CP group, the high levels of TBARS ($p < 0.00001$) were indicative of severe oxidative damage and an increase in lipid peroxidation. Both treatment groups (NAC and TAE) significantly reduced TBARS levels ($p < 0.05$) compared to the CP group, but TAE remained slightly higher than NAC in reducing TBARS-induced oxidative damage, which is indicative of a moderate but noteworthy reduction in oxidative damage. Section (C) shows the total antioxidant capacity (TAC) across the four experimental groups. TAC was substantially lowered in the CP group ($p < 0.0001$) which demonstrated the depletion of overall antioxidant defenses of the cell due to accumulation of oxidative damage. On the other hand, both treatment groups showed strong mitigation of oxidative stress by increasing TAC levels towards the CN baseline, where NAC seemed most effective ($p < 0.00001$) in restoring cellular antioxidant capacities. TAE shows a moderate effect compared to the CP group ($p < 0.00001$) but to a lesser degree than NAC, which is suggestive of partial alleviation of oxidant load. NAC showed robust antioxidant protection in the treatment group while TAE offers moderate but significant improvements across most parameters. The significant oxidative damage and reduced antioxidant capacity in the CP group confirm the detrimental effects of acetaminophen-induced toxicity, which NAC significantly mitigated as standard treatment and TAE as herbal treatment, both returning the diseased state near to baseline (CN group).

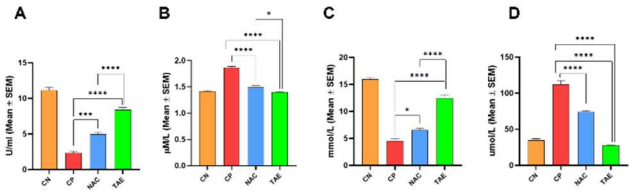

Fig. 3: Effects of different treatments on oxidant status and antioxidant capacity.
(A) Superoxide Dismutase (SOD) Activity, (B) Thio-barbituric Acid Reactive Substances (TBARS), (C) Total Antioxidant Capacity (TAC), (D) Total Oxidant Status (TOS). Data are presented as Mean ± SEM. *Statistical significance is denoted as *p<0.05, **p<0.01, ***p<0.001, ****p<0.0001, ns=p>0.05 (not significant)*

Gene expression analysis

Oxidative stress regulation

In fig. 4, Sections (A) and (B) denote the oxidative stress markers (Keap1 and Nrf2) in liver injury induced by acetaminophen toxicity. Section (A) shows the genetic

expression and fold change (Mean ± SEM) of Keap1. Keap1 sequesters Nrf2 and promotes its degradation, thus acting as an inhibitor of the antioxidant response brought upon by Nrf2 (Ke *et al*., 2013). The CP group showed a marked upregulation in Keap1 expression, which is suggestive of suppression of antioxidant pathways. Conversely, both treatment groups significantly reduced ($p < 0.001$ vs CP) Keap1 levels, indicating a partial restoration of normal cell survival and antioxidant control. The TAE group showed a better restoration towards normality compared to the NAC group, which is suggestive of *T. arjuna*'s protective role in rejuvenating antioxidant stores of the cell. Section (B) shows Nrf2 activity across four experimental groups. Nrf2 acts as a master regulator of antioxidant pathways (Vomund *et al*., 2017) and in the CP group, its activity was diminished, which reflected an imbalance in cellular antioxidant potential under toxic stress. Treatment with NAC subsequently upregulated the expression level of Nrf2 ($p < 0.05$ vs CP) but treatment with TAE showed stronger effects nearing CN levels ($p < 0.0001$ vs CP).

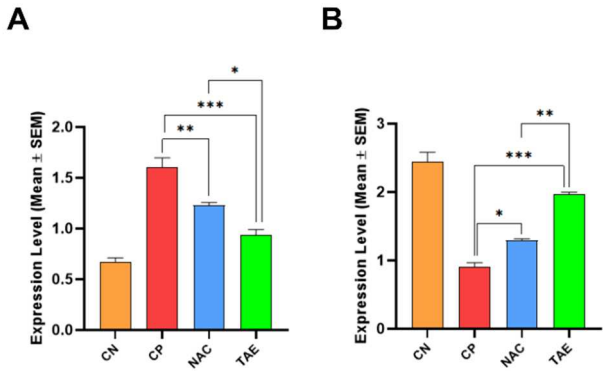

Fig. 4: Gene expression patterns across four experimental groups. (A) Keap1, (B) Nrf2.

To investigate the effects of treatment and acetaminophen toxicity on hepatoprotective mechanisms, mRNA isolation and gene expression levels of key oxidative and proliferative markers were assessed through qRT-PCR. *Statistical significance is denoted as *p<0.05, **p<0.01, ***p<0.001, ****p<0.0001, ns=p>0.05 (not significant)*

UPR signaling pathway molecules

The basic cell signaling molecules that influence directly or indirectly endoplasmic reticulum functioning and protein folding are ERK, JNK, AKT and PPAR-α. In fig. 5, panel (A) shows the expression levels of ERK. The CP group showed a significant increase ($p < 0.01$ vs CN) in the ERK expression, which is explained as a stress-dependent response and upregulation of this gene mediates the release of certain inflammatory cytokines. Treatment with NAC and TAE substantially reduces ERK expression relative to the CP group ($p < 0.01$ vs CP) but therapeutic efficacy between these two treatments was statistically non-significant ($p > 0.05$ = ns). Panel (B) shows the expression levels of JNK, which is a key driver of apoptosis in acetaminophen-induced liver injury. In the CP group, the expression level of JNK is significantly elevated ($p < 0.001$ vs CN) which explains the activation of pro-apoptotic cellular pathways during acetaminophen toxicity and UPR. NAC and TAE treatments both significantly reduce JNK expression ($p < 0.0001$ vs CP). Notably, TAE shows a better effect in reducing JNK expression level compared to NAC, marking its anti-apoptotic effects in imbalanced proteostasis and cellular stress. Panel (C) shows PPAR-α expression across four experimental groups. In the CP group, there was a significant upregulation of PPAR-α expression ($p < 0.0001$ vs CN). The upregulation in PPAR-α expression on sub-cellular levels may be indicative of coping mechanisms against metabolic stress induced by acetaminophen. The acute toxicity raised the levels of PPAR-α as a defense mechanism of cells to cope with the accumulated misfolded/unfolded proteins in the cell matrix. The significant decrease in the expression level of PPAR-α in the NAC treatment groups ($p < 0.0001$ vs CP) is suggestive of the mitigation of initial stress caused by acetaminophen toxicity. A similar effect was seen in the TAE group, where a significant decrease in PPAR-α expression was seen ($p < 0.0001$ vs CP), but mutual effects between the NAC group and the TAE group were statistically non-significant ($p > 0.05$ = ns). Panel (D) shows AKT expression across experimental groups. AKT, alike PPAR-α, is activated as a pro-survival molecule. In the CP group, a significant increase in AKT expression ($p < 0.001$ vs CN) conforms to the activation of cellular coping mechanisms against apoptotic signals triggered by JNK and cytokine storm. Treatment with NAC and TAE improved cellular survival which resulted in substantial downregulation of AKT signaling ($p < 0.001$ vs CP), but a lesser decrease in AKT signaling was seen in the NAC group which was deemed statistically non-significant ($p > 0.05$ = ns).

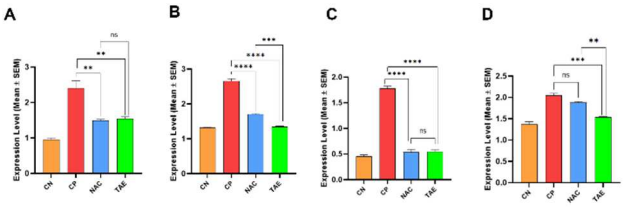

Fig. 5: Hepatic gene expression profiles of key UPR and survival signaling molecules in experimental groups.

(A) ERK, (B) JNK, (C) PPAR-α, (D) AKT. *Statistical significance is denoted as *p<0.05, **p<0.01, ***p<0.001, ****p<0.0001, ns=p>0.05 (not significant)*

Histopathology

Histopathological examination of liver sections was conducted using routine Hematoxylin and Eosin (H&E) staining. The photomicrographs were acquired at 400x magnification to assess hepatic architecture, inflammatory cell infiltration (neutrophil load) and overall cellular integrity.

Panel (A) shows the liver tissue section obtained from the CN group and represents a healthy baseline of hepatic tissue. Overall tissue organization in the CN group shows well-organized centrilobular structures with clearly visible sinusoids lined by endothelial cells and no cellular congestion or nuclear degeneration. Hepatocytic morphology shows polygonal hepatocytes with round, central nuclei and intact cytoplasm with minimal to no inflammatory infiltrate. In fig. 6-A, the black arrow points to the central vein, the blue arrow highlights a normal sinusoid through which blood flows through capillary cords and the pink arrow indicates morphologically intact hepatocytes in a typically polygonal shape and centrally placed nuclei with clear cytoplasm.

Panel (B) shows the liver tissue section from the CP group. There is evidence of architectural disruption where the regular hepatocytic arrangement is lost in the centrilobular region with focal necrotic areas and degeneration of hepatocytes. Marked inflammatory cell infiltrate is visible with sinusoidal congestion, which reflects an acute inflammatory response. Some hepatocytes appear strikingly eosinophilic with pyknotic (condensed or dissolved) nuclei, indicating cell death. In fig. 6-B, the black arrow shows a congested sinusoid reflecting vascular hemorrhage consistent with APAP toxicity. The blue arrow points to vacuolated hepatocytes indicating cellular swelling and onset of apoptosis. The pink arrow shows necrotic hepatocytes characterized by disoriented or dissolved cellular structure.

Panel (C) shows the liver tissue section from the NAC group, where a decrease in necrotic foci is visible compared to the CP group and liver architecture is improved, though not entirely normal. Fewer inflammatory cells infiltrate the tissue and better hepatocytic viability is observed, although some residual signs of injury persist. Such hepatocytic repair depicts the restorative ability of N-acetylcysteine in replenishing GSH stores and decreasing oxidative damage, thereby reducing hepatocellular injury. In fig. 6-C, the black arrow points to the residual area of hepatocellular damage, indicating mild necrosis and ongoing but reduced injury. The blue arrow highlights a region of improved hepatocytes with better nuclear morphology suggestive of partial restoration of liver architecture. The pink arrow points to a sinusoidal space with mild inflammatory focus showing some evidence of congestion.

Panel (D) shows the liver tissue section from the TAE group. The hepatocytes in this section appear more orderly and closer in appearance to the radial arrangement as in the CN group. Central vein and hepatic sinusoids are defined with minimal congestion. The inflammatory infiltrates are substantially reduced and a majority of hepatocytes exhibit normal nuclear morphology with fewer signs of nuclear necrosis. Notable restoration of liver histoarchitecture is observed, which is suggestive of effective hepatoprotection offered by *T. arjuna* extract, likely through antioxidant and anti-inflammatory mechanisms associated with the herbal extract constituents. In fig. 6-D, the black arrow signifies a focal region of well-organized liver parenchyma, which is indicative of the overall recovery of liver tissue compared to the untreated toxic group. The blue arrow points to a sinusoidal space with minimal inflammatory infiltrate, suggestive of cellular clearance. The pink arrow indicates healthy hepatocytes with round nuclei and clear, well-preserved cytoplasm.

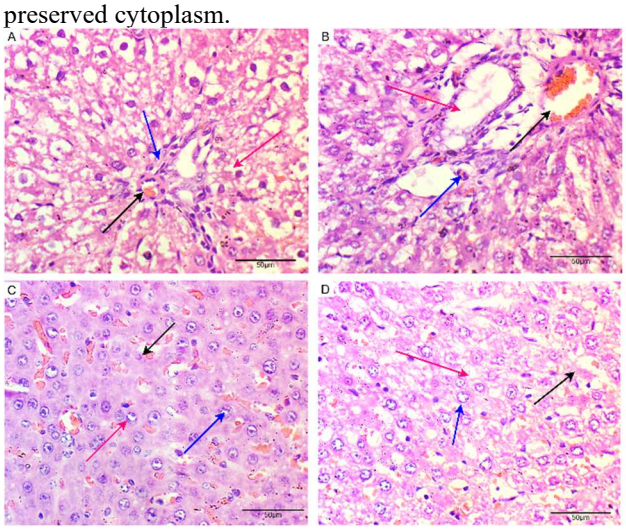

Fig. 6: Histopathological assessment of liver tissue across experimental groups. (A) CN, (B) CP, (C) NAC, (D) TAE. Histological analysis of liver sections was performed using routine Hematoxylin and Eosin (H&E) staining. Representative micrographs were taken at 400× magnification to evaluate hepatic architecture, inflammatory infiltration, and cellular integrity. The black, blue, and pink arrows show key hepatic tissue structures that show substantial architectural changes after toxic induction and treatment.

DISCUSSION

Acetaminophen-induced hepatotoxicity remains a significant concern due to its potential to cause acute liver injury by initializing oxidative stress pathways, mitochondrial dysfunction and endoplasmic reticulum stress-mediated apoptosis (Zhang *et al*., 2022). The liver, being the major site for most drug biotransformation that goes through first-pass hepatic metabolism, remains a target for drug-induced injury and a site of initiation for cellular stress (Luo *et al*., 2023). In this study, the protective effects of *T. arjuna* extract against APAP-induced liver injury were evaluated using serological, histopathological and molecular analyses.

Acetaminophen overdose is widely recognized as a major cause of liver damage, with its hepatotoxic effects well documented in both clinical and experimental studies (Yan *et al*., 2018). The current study's findings regarding increased levels of liver function markers such as ALT,

AST and bilirubin are consistent with those of Ullah *et al*., (2022), who reported similar elevations in these markers as indicators of paracetamol-induced liver injury. Comparable results were also observed by Khan *et al*., (2023), where ALT and AST levels significantly increased following paracetamol induction. Histologically, the observed necrotic changes in hepatic tissues align with the findings of Islam *et al*., (2021), who reported coagulative necrosis and inflammatory residues in the acetaminophen-toxic group.

Oxidative stress and antioxidant defense

The initial biological response to metabolic or pathological threats involves the production of reactive oxygen and nitrogen species (ROS and RNS) to facilitate pathogen destruction and initiate inflammation for immune cell recruitment (Zhang and Kaufman, 2008). However, when the stressor persists, this response becomes pathological, leading to excessive ROS/RNS production that damages host cells and tissues (Yang *et al*., 2016). In acetaminophen-induced hepatotoxicity, ROS generation depletes endogenous antioxidants like GSH, disrupts mitochondrial function and triggers ER stress due to the accumulation of misfolded proteins (Wu and Kaufman, 2006; Xiao *et al*., 2020). In the current study, elevated TOS and decreased SOD levels in the APAP-treated group confirmed excessive ROS generation and oxidative imbalance (Du *et al.,* 2025). These findings are consistent with Jaeschke and Ramachandran (2020), who reported P450-mediated ROS overproduction in APAP toxicity leading to lipid peroxidation and necrosis. The decrease in SOD, consistent with Du *et al*. (2017), reflects an overwhelmed antioxidant defense system. Increased TBARS levels further support the initiation of apoptotic pathways, aligning with Jaeschke *et al*. (2019). Importantly, both NAC and *T. arjuna* bark extract (TAE) treatments reversed these effects, but TAE showed superior efficacy in restoring antioxidant activity. While NAC is the standard treatment for APAP overdose (Teschke and Danan, 2020), its limitations such as delayed hepatocyte regeneration and reduced bioavailability over time (Yang *et al*., 2009) highlight the novelty of TAE treatment. The current findings suggest that TAE's polyphenolic content may confer additional antioxidant mechanisms beyond GSH replenishment offered by NAC (El-Serafi *et al*., 2018; Manna *et al*., 2006). This positions *T. arjuna* as a promising alternative or complementary therapy for APAP-induced liver injury, with potential advantages in efficacy and sustained antioxidant response.

Effects on critical regulators of cellular stress response

The Keap1-Nrf2 pathway is a critical regulator of cellular oxidative stress response. Keap1 interacts with Nrf2 as a master regulator of cellular redox equilibrium and under physiological conditions, Keap1-Nrf2 complex signaling induces ubiquitination of Nrf2 to activate ARE, which scavenges free radicals and regulates the oxidant load of the cells (Ke *et al*., 2013). In this study, Keap1 was significantly upregulated in the CP group likely due to oxidative stress-induced feedback regulation. Elevated Keap1 restricts Nrf2 activation, which is shown by decreased Nrf2 expression in the CP group, leading to diminished antioxidant defense. Conversely, both NAC and TAE-treated experimental units showed elevated levels of Nrf2 and decreased genetic expression of Keap1, which suggests the relapse of cellular defense mechanisms. TAE treatment in particular decreased Keap1 level to near-normal boundary, suggesting that the bioactive elements of whole extract possess oxidant inhibition properties which enhance Nrf2-driven antioxidant responses, thus mitigating liver injury due to oxidative stress. The upregulation of Nrf2 in the TAE group suggests direct activation of cytoprotective pathways and inhibition of Keap1, thereby enhancing cellular resilience. Similar effects were seen in a study by Im *et al*., (2012) where thioredoxin 1 expression was correlated with Nrf2 pathways in cell survival mechanisms of cancer cells.

Involvement of UPR signaling molecules in different facets of stress response

Mitogen-Activated Protein Kinases (MAPK) are a class of special proteins which are directly involved and activated during ER stress and facilitate the signaling of UPR (Altarjami, 2025). When unfolded proteins accumulate in the ER, IRE1, which is an ER stressor, binds to second messenger proteins, which subsequently activate JNK (Zhang *et al*., 2022). Once JNK is activated, the cellular survival threshold is tilted towards cell death when ERS is severe. In the current study, the APAP toxic group (CP) showed upregulated JNK levels due to increased ROS, glutathione depletion and accumulation of reactive metabolites that led to the activation of necrotic pathways in hepatocytes, exacerbating liver injury. A similar upregulation as seen in ERK levels in the CP group, which correlated to UPR signaling through a different pathway but provides a cell survival and repair output. Treatment with *T. arjuna* substantially decreased the upsurge of apoptotic signals by downregulating ERK and JNK expression levels, which were backed by reduced oxidative stress due to the anti-oxidant powers of the herbal extract. PPAR-α is a classical sensor of lipid peroxidation due to ROS generation and its upregulation is directly related to ROS-mediated fatty-acid oxidation of hepatocytic membrane (Zhao *et al*., 2017). In the CP group, PPAR-α levels were upregulated, which indicated severe lipid peroxidation due to NAPQI. ER stress altered lipid metabolism of cells and upregulated PPAR-α levels assisted in coping with lipid by-product overload, plausibly by regulating genes involved in β-oxidation as a compensatory mechanism (Lin *et al*., 2022). The key active ingredient of *T. arjuna* extract is Arjunolic acid, which is a triterpenoid saponin and is reported as a PPAR-α agonist (Bansal *et al*., 2017). The specific effects of *T. arjuna* on basal metabolic activity of PPAR-α in hepatocytes of toxic group treated with TAE were thus evaluated and the observations showed promising results in ameliorating APAP-toxicity in hepatocytes along with vital antioxidant

and anti-inflammatory properties. Similarly, AKT is a crucial kinase in the PI3K/AKT pathway, also a subdivision of the UPR signaling cascade, which is responsible for regulating cell survival and proliferation (He *et al*., 2021). AKT upregulation in the APAP-toxic group may be explained as an initial pro-survival response of the cell to counteract oxidative damage and apoptotic signals. Excessive AKT upregulation had a resultant aberrance in cell survival signals which put the hepatocytes in a fibrotic cycle, as is evident from histopathological findings where necrotic mass and liquefaction of cell membrane with irregular cytoplasmic contents were seen in the CP group. This finding is also supported by Liu *et al*., (2020) in their study to investigate the PI3K/AKT pathway modulation in multidrug resistance of cancers. The TAE group in the current study shows AKT downregulation, which can be explained by the close linkage of AKT signaling with inflammatory signaling pathways through NF-κB activation and cytokine recruitment (Liu *et al*., 2020), hence the anti-inflammatory effects of *T. arjuna* also modulate this key genetic interplay.

The findings of the current study demonstrate that TAE effectively modulates these pathways, restoring cellular homeostasis and offering hepatoprotective effects comparable to the standard treatment, N-acetylcysteine. Notably, the effect of TAE on the expression level of cell proliferation markers and UPR signaling molecules suggests a novel role in liver regeneration and restoration of cellular equilibrium after the accumulation of toxic metabolites, warranting further investigation. While these results provide promising evidence for *T. arjuna* as a potential therapeutic agent, additional studies are needed to elucidate its precise molecular mechanisms, optimize dosing strategies and validate its efficacy in clinical settings. Future research should also explore its long-term safety profile and potential synergistic effects with existing hepatoprotective agents.

Acknowledgments
The authors are grateful to the Institute of Physiology and Pharmacology, University of Agriculture Faisalabad, for assisting and providing guidance throughout the research period. The authors would also like to express sincere gratitude to Dr. Muhammad Naeem Faisal (Associate Professor – Institute of Physiology and Pharmacology, University of Agriculture Faisalabad) for his invaluable guidance, insightful feedback, and continuous support throughout the development of this work.

Authors' contributions
Writing – Original Draft: W.N.
Writing – Review and Editing: W.N., B.A.
Conceptualization: S.U.H., W.N., B.A., W.M.
Formal Analysis: W.N., W.M.
Data Curation: W.N., S.U.H, W.M.
Investigation: W.N., S.U.H., B.A.
Methodology: W.N., S.U.H.
Supervision: S.U.H., B.A., W.M.

Funding
None

Data availability statement
The data supporting the findings of this study are available from the corresponding author upon reasonable request.

Ethical approval
All animal experiments were performed in the accredited animal research facility at the University of Agriculture Faisalabad, Pakistan and comply with Bioethics Protocols (D. No. 1982/ORIC) issued by the Institutional Biosafety and Bioethics Committee of the Office of Research, Innovation and Commercialization (ORIC), University of Agriculture Faisalabad.

Conflict of interest
The authors declare that they have no conflicts of interest, financial or otherwise, related to this study.

REFERENCES

Ahmad M, Tahir M, Hong Z, Zia MA, Rafeeq H, Ahmad MS, Rehman SU and Sun J (2025). Plant and marine-derived natural products: Sustainable pathways for future drug discovery and therapeutic development. *Front. Pharmacol.*, **15**: 1497668.

Alamri ZZ (2018). The role of liver in metabolism: An updated review with physiological emphasis. *Int. J. Basic Clin. Pharmacol.*, **7**: 2271.

Altarjami LR (2025). Anticancer and antioxidant activities of polyphenolic pomegranate peel extracts obtained by a novel hybrid ultrasound-microwave method: In vitro and in vivo studies in albino mice with HeLa, colon, and HepG2 cancerous cell lines. *Pak. Vet. J.*, 45(2): 723-734. http://dx.doi.org/10.29261/pakvetj/2025.154

Andrade RJ, Aithal GP, Bjornsson ES, Kaplowitz N, Kullak-Ublick GA, Larrey D and Karlsen TH (2019). EASL Clinical practice guidelines: Drug-induced liver injury. *J. Hepatol*., **70**: 1222-1261.

Bansal T, Chatterjee E, Singh J, Ray A, Kundu B, Thankamani V, Sengupta S and Sarkar S (2017). Arjunolic acid, a peroxisome proliferator-activated receptor α agonist, regresses cardiac fibrosis by inhibiting non-canonical TGF-β signaling. *J. Biol. Chem.*, **292**: 16440–16462.

Chalasani NP, Hayashi PH, Bonkovsky HL, Navarro VJ, Lee WM and Fontana RJ (2014). ACG clinical guideline: The diagnosis and management of idiosyncratic drug-induced liver injury. *Am. J. Gastroenterol.*, **109**: 950-966.

Dogan M, Oz ME and Akbaba S (2025). One-Run qPCR assays for identification of domestic ruminant abortion: verification and application process. *Pak. Vet. J.*, **45**(2): 553-565. http://dx.doi.org/10.29261/pakvetj/2025.181

Du K, Farhood A and Jaeschke H (2017). Mitochondria-targeted antioxidant Mito-Tempo protects against acetaminophen hepatotoxicity. *Arch. Toxicol.,* **91**: 761-773.

Du X, Maqbool B, Shichiyakh R, Haque MA, Aubakirov M, Syamsu JA and Khan A (2025). Eubiotics improve gut health and overall production in animals by reducing pathogenic bacteria. *Pak. Vet. J.*, **45**(2): 488-498.

El-Serafi I, Remberger M, El-Serafi A, Benkessou F, Zheng W, Martell E, Ljungman P, Mattsson J and Hassan M (2018). The effect of N-acetyl-l-cysteine (NAC) on liver toxicity and clinical outcome after hematopoietic stem cell transplantation. *Sci. Rep.,* **8**: 8293.

Ghosh J, Das J, Manna P and Sil PC (2010). Protective effect of the fruits of Terminalia arjuna against cadmium-induced oxidant stress and hepatic cell injury via MAPK activation and mitochondria dependent pathway. *Food. Chem.,* **123**: 1062-1075.

Green MD, Shires TK and Fischer LJ (1984). Hepatotoxicity of acetaminophen in neonatal and young rats. *Toxicol. Appl. Pharmacol.,* **74**: 116-124.

He Y, Sun MM, Zhang GG, Yang J, Chen KS, Xu WW and Li B (2021). Targeting PI3K/Akt signal transduction for cancer therapy. *Signal Transduct. Target Ther.,* **6**: 425.

Hosack T, Damry D and Biswas S (2023). Drug-induced liver injury: A comprehensive review. *Therap. Adv. Gastroenterol.,* **16**.

Hu H, Tian M, Ding C and Yu S (2019). The C/EBP Homologous Protein (CHOP) Transcription factor functions in endoplasmic reticulum stress-induced apoptosis and microbial infection. *Front. Immunol.,* **9**.

Im JY, Lee KW, Woo JM, Junn E and Mouradian MM (2012). DJ-1 induces thioredoxin 1 expression through the Nrf2 pathway. *Hum. Mol. Genet.,* **21**: 3013-3024.

Iorga A, Dara L and Kaplowitz N (2017). Drug-induced liver injury: Cascade of events leading to cell death, apoptosis or necrosis. *Int. J. Mol. Sci.,* **18**: 1018.

Jaeschke H and Ramachandran A (2020). The role of oxidant stress in acetaminophen-induced liver injury. *Curr. Opin. Toxicol.,* 20–21, 9–14.

Jaeschke H, Ramachandran A, Chao X and Ding WX (2019). Emerging and established modes of cell death during acetaminophen-induced liver injury. *Arch. Toxicol.,* **93**: 3491-3502.

Katarey D and Verma S (2016). Drug-induced liver injury. *Clin. Med.,* **16**: 104-109.

Ke B, Shen XD, Zhang Y, Ji H, Gao F, Yue S, Kamo N, Zhai Y, Yamamoto M, Busuttil RW and Kupiec-Weglinski JW (2013). KEAP1-NRF2 complex in ischemia-induced hepatocellular damage of mouse liver transplants. *J. Hepatol.,* **59**: 1200-1207.

Kong Q, Shang Z, Liu Y, Fakhar-e-Alam Kulyar M, Suolang S, Xu Y, Tan Z, Li J and Liu S (2023). Preventive effect of *Terminalia bellirica* (Gaertn.) Roxb. extract on mice infected with Salmonella Typhimurium. *Front. Cell. Infect. Microbiol.,* **12**.

Lin Y, Wang Y and Li P (2022). PPARα: An emerging target of metabolic syndrome, neurodegenerative and cardiovascular diseases. *Front. Endocrinol. (Lausanne).,* **13**.

Liu R, Chen Y, Liu G, Li C, Song Y, Cao Z, Li W, Hu J, Lu C and Liu Y (2020). PI3K/AKT pathway as a key link modulates the multidrug resistance of cancers. *Cell Death Dis.,* **11**: 797.

Luo G, Huang L and Zhang Z (2023). The molecular mechanisms of acetaminophen-induced hepatotoxicity and its potential therapeutic targets. *Exp. Biol. Med.,* **248**: 412–424.

Mandal S, Patra A, Samanta A, Roy S, Mandal A, Mahapatra T, Das Pradhan S, Das K and Nandi DK (2013). Analysis of phytochemical profile of *Terminalia arjuna* bark extract with antioxidative and antimicrobial properties. *Asian Pac. J. Trop. Biomed.,* **3**: 960–966.

Manna P, Sinha M, Pal P and Sil PC (2007). Arjunolic acid, a triterpenoid saponin, ameliorates arsenic-induced cyto-toxicity in hepatocytes. *Chem. Biol. Interact.,* **170**: 187-200.

Manna P, Sinha M and Sil PC (2006). Aqueous extract of *Terminalia arjuna* prevents carbon tetrachloride induced hepatic and renal disorders. *BMC Complement. Altern. Med.,* **6**: 33.

Paridaens A, Raevens S, Colle I, Bogaerts E, Vandewynckel Y, Verhelst X, Hoorens A, van Grunsven LA, Van Vlierberghe H, Geerts A and Devisscher L (2017). Combination of tauroursodeoxycholic acid and N-acetylcysteine exceeds standard treatment for acetaminophen intoxication. *Liver Int.,* **37**: 748-756.

Rao J, Zhang C, Wang P, Lu L, Qian X, Qin J, Pan X, Li G, Wang X and Zhang F (2015). C/EBP homologous protein (CHOP) contributes to hepatocyte death via the promotion of ERO1α signalling in acute liver failure. *Biochem. J.,* **466**: 369-378.

Rui L (2014). Energy Metabolism in the Liver, in: *Comprehensive Physiology. Wiley*, 177-197.

Saito C, Zwingmann C and Jaeschke H (2010). Novel mechanisms of protection against acetaminophen hepatotoxicity in mice by glutathione and N-acetylcysteine. *Hepatology* **51**: 246-254.

Teschke R and Danan G (2020). Worldwide use of RUCAM for causality assessment in 81,856 idiosyncratic DILI and 14,029 HILI Cases published 1993–Mid 2020: A comprehensive analysis. *Medicines* **7**: 62.

Tsai MC and Huang TL (2015). Thiobarbituric acid reactive substances (TBARS) is a state biomarker of oxidative stress in bipolar patients in a manic phase. *J. Affect. Disord*., **173**: 22–26.

Tsai MS, Liou GG, Liao JW, Lai PY, Yang DJ, Wu SH and Wang SH (2024). N-acetyl cysteine overdose induced acute toxicity and hepatic microvesicular steatosis by disrupting gsh and interfering lipid metabolisms in normal mice. *Antioxidants,* **13**: 832.

Uzi D, Barda L, Scaiewicz V, Mills M, Mueller T, Gonzalez-Rodriguez A, Valverde AM, Iwawaki T, Nahmias Y, Xavier R, Chung RT, Tirosh B and Shibolet O (2013). CHOP is a critical regulator of acetaminophen-induced hepatotoxicity. *J. Hepatol.,* **59**: 495-03.

Vomund S, Schafer A, Parnham M, Brüne B and Von Knethen A (2017). Nrf2, the Master Regulator of Anti-Oxidative Responses. *Int. J. Mol. Sci.,* **18**: 2772.

Wu J and Kaufman RJ (2006). From acute ER stress to physiological roles of the unfolded protein response. *Cell Death Differ.,* **13**: 374-384.

Xiao T, Liang X, Liu H, Zhang F, Meng W and Hu F (2020). Mitochondrial stress protein HSP60 regulates ER stress-induced hepatic lipogenesis. *J. Mol. Endocrinol.,* **64**: 67-75.

Yang R, Miki K, He X, Killeen ME and Fink MP (2009). Prolonged treatment with N-acetylcystine delays liver recovery from acetaminophen hepatotoxicity. *Crit. Care.,* **13**: R55.

Yang X, Srivastava R, Howell SH and Bassham DC (2016). Activation of autophagy by unfolded proteins during endoplasmic reticulum stress. *Plant. J.,* **85**: 83-95.

Zhang J, Guo J, Yang N, Huang Y, Hu T and Rao C (2022). Endoplasmic reticulum stress-mediated cell death in liver injury. *Cell Death Dis.,* **13**: 1051.

Zhang K and Kaufman RJ (2008). From endoplasmic-reticulum stress to the inflammatory response. *Nature* **454**: 455-462.

Zhao Q, Yang R, Wang J, Hu DD and Li F (2017). PPARα activation protects against cholestatic liver injury. *Sci. Rep.,* **7**: 9967.